Differential Cytotoxicity of Metal Oxide Nanoparticles

J. Chen*†, J. Zhu*†, H.-H. Cho**, K. Cui*, F. Li*, X. Zhou*, J.T. Rogers**, S.T.C. Wong* and X. Huang*,**

*Functional and Molecular Imaging Center, Department of Radiology, Brigham and Women's Hospital and Harvard Medical School, USA, xhuang3@partners.org
**Neurochemistry Laboratory, Department of Psychiatry and Genetics & Aging Research Unit, Massachusetts General Hospital and Harvard Medical School, USA.
†Equal Contribution

ABSTRACT

Concerns about potential health hazard of nanomaterials are growing. To determine the potential toxicity of metal oxide nanoparticles, human SH-SY5Y neuroblastoma and H4 neuroglioma cells were exposed to Fe_2O_3, CuO, and ZnO nanoparticles and their metal ion counterparts (Fe^{3+}, Cu^{2+}, and Zn^{2+}) at a concentration range of 0.01-100 μM for 48 hours, under the cell culture conditions: 95% O_2, 5% CO_2, 85% humidity, 37°C. Their ensemble cell viability was determined by MTS cell proliferation assays. A live/dead cell assay was also performed, and cellular images were acquired by a high-content fluorescence microscope and quantified by a novel computerized image analysis protocol. Our data indicated that exposure of these nanoparticles induced differential toxic effects in both SH-SY5Y and H4 cells, and the cells had dose-dependent toxic responses to the CuO nanoparticle insult. In conclusion, toxic responses of the nanoparticles are complex, and they warrant further *in vivo* studies.

Keywords: metal oxide nanoparticles, cytotoxicity, high-content cell imaging, SH-SY5Y neuroblastoma cell, H4 neuroglioma cell

1 INTRODUCTION

Nanoparticles (<100 nm in diameter) exhibit unique physicochemical properties and can have many unknown biological effects. Although the nanostructured materials hold promises for many industrial and biomedical applications, there are growing concerns among the general public and regulators about their potential health hazard. Studies in epidemiology consistently show that enhanced exposures of sub-micro atmospheric particulates lead to short-term increases in morbidity and mortality [1]. There are evidences indicate that ultrafine diesel exhaust particles (DEP) that are taken up by human airway epithelial cells in vitro [2], increase cytokine production such as IL-8, growth related oncogene-α (GROα), and granulocyte macrophage colony-stimulating factor (GM-CSF) [3,4], as well as evoke inflammatory responses in human airway epithelium [5]. In addition, other adverse health effects have been described in relevant studies.

Recently, nanocarrier-based CNS delivery systems have been proposed for enhancing drug transport into the central nervous system (CNS) [6]. However, toxicity and brain distribution profiles of nanoparticles must be considered as they can alter blood-brain barrier integrity and permeability [7]. Therefore study on the potentially toxic responses of nanoparticles is very important for monitoring their safe use. In particular, the cytotoxicity data of metal oxide nanoparticles for brain cells, which are essential for nanomaterial risk assessment, are sparse [8, 9]. In this study, cell models of human SH-SY5Y neuroblastoma and H4 neuroglioma cells were exposed to Fe_2O_3, CuO, and ZnO nanoparticles and their metal ion counterparts, MTS and live/dead assays were performed for their cell viability profiles. High-content cellular fluorescent images were acquired with a fluorescence microscope. These high-content images were analyzed by a data-driven background algorithm and imaging modality that has been developed for live/dead cell imaging assay. Our results suggested CuO nanoparticles engendered significant dose-dependent cell death in both H4 and SH-SY5Ycells (more strikingly), while cytotoxic effects of Fe_2O_3 and ZnO nanoparticles were marginal compared to the controls. These results suggest that further studies are required to assess the potential health risks of manufactured nanoparticles.

2 MATERIALS AND METHODS

2.1 Cell culture and Reagents

Human SH-SY5Y neuroblastoma and H4 neuroglioma cells from the ATCC (Manassas, VA) were employed as cell models. Cells ($2x10^4$) were seeded into 96-well cell culture microplates and cultured in Dubelcco's Modified Eagle Medium (DMEM, Gibco) supplemented with 10% fetal bovine serum (Sigma), 2 mM L-glutamine and 1% antibiotics (100 U/mL penicillin + 100 g/mL streptomycin, Gibco). These cells were incubated for 48 hours under the cell culture conditions (95% O_2, 5% CO_2, 85% humidity, 37ºC), together with Fe_2O_3 (2-25 nm in diameter), CuO (≈33 nm in diameter), and ZnO (50-70 nm in diameter) nanoparticles (Sigma-Aldrich) at a concentration range of 0.01-100 μM, which were diluted from nanoparticle/DMSO stock solutions. To minimize DMSO toxicity, the 1000X

NSTI-Nanotech 2007, www.nsti.org, ISBN 1420061836 Vol. 2, 2007

nanoparticle/DMSO stock solutions for every tested nanoparticle concentration were used such that DMSO concentration in each well was ≤ 0.1%. 0.1% DMSO alone was used as background control.

2.2 MTS Assay

MTS assay of cell viability was performed with the CellTiter 96® AQ_{ueous} One Solution Cell Proliferation Assay kit (Promega, Madison, WI). After a 48 hour treatment of metal oxide nanoparticles, 20 µL/well of the MTS reagent was added to 100 µL of sample in each well of 96-well microplates and allowed to incubate for 1 hour at 37°C in a humidified, 5% CO_2 atmosphere. The absorbance of the samples was then taken at a wavelength of 490 nm. Cell viability was expressed as a percentage of the untreated controls. Results were expressed as mean ± SE.

2.3 Live/Dead Fluorescence Assays

The cytotoxic effects of the nanoparticles were also evaluated using live/dead fluorescence assays (Molecular Probes/Invitrogen). Hoechst, Calcein AM, Ethidium homodiner 1 dyes (Molecular Probes/Invitrogen, Eugene, OR) were used for total, live, and deal cell nucleic staining, respectively. After 48 hours treatment with Fe_2O_3, CuO, and ZnO nanoparticles, these dyes (in each well: 2 µM of Calcein AM, 4 µM of Ethidium homodiner1, and 5 µg/mL of Hoechst dye) were added into wells. The cells were incubated with the dyes for 45 minutes at 37 °C in the tissue culture incubator. High-content cellular images were captured by GE IN Cell Analyzer 1000. The followings are optimal excitation/emission wavelengths for acquiring fluorescent cellular images: Ex 475 nm/Em 535 nm for Calcein AM-stained live cells; Ex 535 nm/Em 620 nm for EthD-1 stained dead cells; and Ex 360 nm/Em 460 nm for Hoechst-stained cells.

2.4 High-content Image Processing

A novel computerized image analysis protocol was developed for quantifying high-content cell images (F Li et al, manuscript is in preparation). It has been applied to process fluorescent cellular images acquired in this study.

In brief, to categorize the live/dead cells and background, a data-driven background correction method used as the threshold technology was included to generate two thresholds. Cellular images were categorized into three classes: bright cells, dark cells, and background. The linear scale-space representation theory that combined the gradient vector flow field for the nuclei detection was applied to profile total cells. Seeded watershed based region-growing algorithm for the cell segmentation, a statistical model based splitting and merging steps were used to offset under-segmentation. This adaptive multiple threshold algorithm entails the following features: (i) Gaussian filtering with proper scale for generation of local image intensity maxima within each cell; (ii) a novel method for defining local image intensity maxima based on the gradient vector field; and (iii) a statistical model for overcoming the cell segmentation problem.

3 RESULTS

3.1 Exposure of Nanoparticles and Their Counterpart Metal Ions Caused Cell Viability Reduction

Cells were exposed for 48 hours in a culture medium containing 0.01, 0.1, 1, 10, 100 µM of metal oxide nanoparticles or their counterpart ions, respectively. The cytotoxicity effects of Fe_2O_3, CuO, and ZnO nanoparticles and their metal ion counterparts upon SH-SY5Y and H4 cells were assessed by MTS assay.

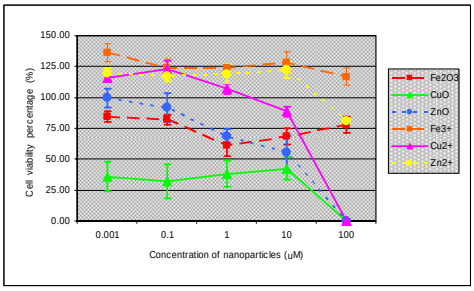

Fig. 1. Cell viability profiles of SH-SY5Y Cells

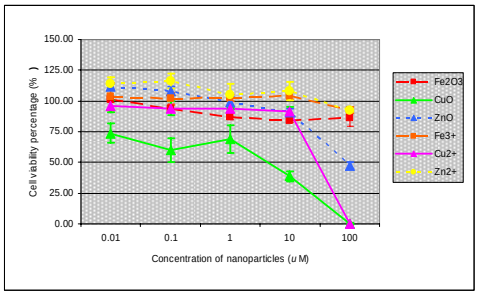

Fig. 2. Cell viability profiles of H4 Cells

Results show (see Fig. 1, Fig. 2) that Fe_2O_3, ZnO nanoparticles had a similar toxicity profiles, while CuO nanoparticles attenuated the cell viability the most after 48 hour treatment. For comparison, the toxic effects of their counterpart metal ions were also determined under the same experimental conditions. The percentages of cell viability based on negative (0.1% DMSO) and positive controls (10% Triton-X) were calculated and graphed. The data indicate the mean±SE (n=5). The decrease of cell viability induced by CuO nanoparticles in SH-ST5Y or in H4 cells are about 60-70% or 25-60% at the concentration of 0.01-10 µM respectively. 100% viabilities loss observed at treatment concentration of 100 µM in both SH-SY5Y and H4 cells. It seemed that the cytotoxic responses of different

cell lines to nanoparticle insults were different. SH-SY5Y cells were more sensitive than H4 cells in this experiment.

3.2 CuO Nanoparticles Engendered Significant Cell Death as Determined by Live/Dead Fluorescence Assays and High-content Image Analysis

To further quantify cytotoxic effects of the metal oxide nanoparticles, live (Calcein-AM positive cell) and dead (Ethidium Homodiner-1 positive cell) assays were performed under the same culture and treatment conditions. The cellular images were captured by the IN Cell Analyzer 1000.

In order to automatically analyze high-content images data at a high throughput manner, image pre-processing steps were taken to remove the noises, artifacts, uneven illumination. A data-driven background algorithm was employed to correct the image degradation originated from uneven illumination and striped patterns. This algorithm was fast, and the resulting images had better quality. After applying Gaussian filter with the proper scale to the images, noises with uniform distribution were effectively suppressed. The cell image segmentation had been converted to the determination of the local intensity maxima from the filtered images. We used the central points to denote the local intensity maxima and put forward a local intensity maxima detection method in which a gradient vector flow field was built. And then cellular image pixels moved in and converged at the central point. Consequently we were able to detect the central points by counting the number of converged pixels. In cell image segmentation, the region-based seeded watershed algorithm was adopted for the statistical modeling of under-segmented objects. This approach had also taken into account of computational efficiency. Our data (not shown) indicated that the automated image analysis protocol can achieve approximately 95% success rate during live/dead cell segmentation and background differentiation compared to manual analysis procedures.

Percentages of live cells over total cells were reported (Fig. 3, Fig. 4 and Fig. 5). The data indicate the mean±SE (n=6). Both H4 and SH-SY5Y cells showed dose-dependent toxic responses to the insults of CuO nanoparticles after 48-hour exposure to the metal oxide nanoparticles. In particular, CuO nanoparticle exposure resulted in a marked decrease of live cells in SH-ST5Y and H4 cells at 100 μM concentration. 60% and 40% drop in live cell percentages have been observed in SH-ST5Y and H4 cells, respectively. These results are in good agreement with ensemble cellular activity measurements. However, Live/Dead-based assays also revealed that there were no statistically significant differences in live/dead cell profiles in SH-ST5Y and H4 cells due to Fe_2O_3 and ZnO treatments (Figs 3 and 5) regardless nanoparticle concentrations.

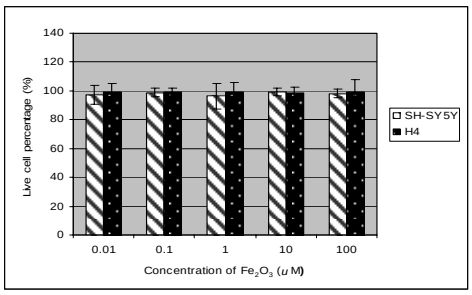

Fig. 3. Cytotoxic effects of Fe_2O_3 nanoparticles on SH-SY5Yand H4 Cells

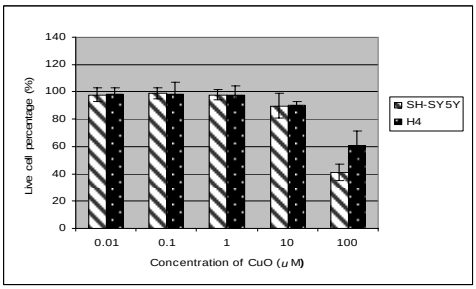

Fig. 4. Cytotoxic effects of CuO nanoparticles on SH-SY5Yand H4 Cells

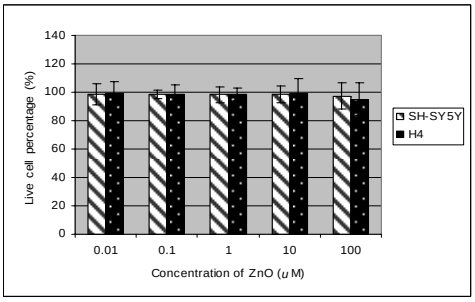

Fig. 5. Cytotoxic effects of ZnO nanoparticles on SH-SY5Yand H4 Cells

4 DISCUSSION

We have first shown that CuO nanoparticles but not Fe_2O_3 and ZnO nanoparticles induced significant decrease of cell viability in SH-SY5Y and H4 cells. And different cell types exhibited various toxic responses to nanoparticles exposure. This means nanopaticles with unique physicochemical properties may pose potential risks to human health [10]. Currently, many consumer products contain nanomaterials such as cosmetics, paints and textiles. However, their toxicological data are very limited. Thus determining the impact of these nanoparticles upon human health is imperative.

Nanomedicine is a rapidly expanding medical research area, promising for revolutionary bioimaging modalities, more efficacious drug delivery and gene therapy with much less side effects [11]. Nevertheless, long-term exposure to

NSTI-Nanotech 2007, www.nsti.org, ISBN 1420061836 Vol. 2, 2007

CdTe quantum dots causes functional impairments in liver cells. Additionally, in human neuroblastoma cells, quantum dot-induced cell death has been found to incur Fas upregulation and lipid peroxidation [12, 13]. Further, a recent publication reported that nanoparticles may be taken up directly into the brain by trans-synaptic transport [14]. And the use of paramagnetic iron oxide nanoparticles as T_2-weighted MRI contrast agent has been proved to be clinically useful [15]. However, their long-term potential adverse effects upon human CNS are not clear.

The underlying molecular mechanism for observed cytotoxic responses of nanoparticles are complicated and not well studied. Nanoparticles can induce oxidative stress in alveolar epithelial cells due to their interactions with cellular components. Such interactions can induce oxidative stress, although not all nanomaterials with various electronic configurations and diverse surface properties will induce spontaneous generation of reactive oxygen species (ROS) [16, 17]. Oxidative stress has been implicated in the pathogenesis of neurodegenerative diseases such as Parkinson's and Alzheimer's diseases [18]. In addition, metal ions such as zinc and copper can interact with both APP and Aβ and potentiate Alzheimer's disease pathogenesis by promoting aggregation of these normal cellular proteins and ROS production [19, 20, 21]. Further, mounting experimental evidence demonstrates that the increased production of free radicals and oxidative damages due to copper dyshomeostasis are involved in many CNS disorders [22]. In the future, it is worthwhile investigating potential pathogenic roles of these metal oxide nanoparticles in neurodegenerative processes.

5 CONCLUSIONS

The data from the present study demonstrate that metal oxide nanoparticle exposure induced differential cytotoxic effects in both SH-SY5Y and H4 cells. In particular, the nanoparticles and their counterpart metal ions had a similar toxicity profiles while CuO nanoparticles and Cu^{2+} attenuated the cell viability the most. Additionally, CuO nanoparticles engendered significant cell death in both H4 and SH-SY5Y cells (more strikingly) while cytotoxic effects of Fe_2O_3 and ZnO nanoparticles were marginal compared to controls. Moreover, our data (not shown) have also indicated that our novel automated image analysis protocol can achieve 95% success rate for live/dead cell and background differentiation compared to manual procedures. Further, our data also imply that neurotoxic responses of nanoparticles are complex, and they warrant further investigation using *in vivo* models. Given their paucity, these toxicity data for nanoparticle will be extremely useful for assessing health risk of nanomaterials.

6 ACKNOWLEDGEMENTS

This work was supported by a NIH Career Development grant (X. Huang, 5K01MH002001) and funds from Radiology Department of Brigham and Women's Hospital, the Center for Bioinformatics Program Grant (S.T.C. Wong) of Harvard Center for Neurodegeneration & Repair. J. Zhu is a recipient of a K12 training grant (D. N. Kennedy, 5K12MH069281).

REFERENCES

[1] P. Borm, D. Robbins, S. Haubold, T. Kuhlbusch, H. Fissan, K. Donaldson, R. Schins, V. Stone, W. Kreyling, J. Lademann, J. Krutmann, D. Warheit and E. Oberdorster, Part Fibre Toxicol, 3,11, 2006.

[2] S. Boland, A. Baeza-Squiban, T. Fournier, O. Houcine, M. Gendron, M. Chevrier, G. Jouvenot, A. Coste, M. Aubier, and F. Marano, Am J Physiol, 276, L604-13, 1999.

[3] S. Salvi, C. Nordenhall, A. Blomberg, B. Rudell, J. Pourazar, F. Kelly, S. Wilson, T. Sandstrom, S. Holgate and A. Frew, Am J Respir Crit Care Med, 161, 550-57, 2000.

[4] S. Boland, V. Bonvallot, T. Fournier, A. Baeza-Squiban, M. Aubier and F. Marano, Am J Physiol Lung Cell Mol Physiol, 278, L25-L32, 2000.

[5] A. Baeza-Squiban, V. Bonvallot, S. Boland and F. Marano, Cell Biol Toxicol, 15, 375-380, 1999.

[6] S. Tiwari and M. Amiji, Curr Drug Deliv, 3(2):219-32, 2006.

[7] P. Lockman, J. Koziara, R. Mumper and D. Allen, J Drug Target, 12(9-10):635-41, 2004.

[8] G. Oberdorster, et al. Part Fibre Toxicol 2, 8, 2005.

[9] M. Wiesner, et al. Environ Sci Technol 40(14), 4336-4345, 2006.

[10] A. Nel, T. Xia, L. Madler and N. Li, Science, 311, 622-627, 2006.

[11] V. Brower, J Natl Cancer Inst, 98, 9-11,2006.

[12] S. Choi, J. Cho, J. Desbarats, J. Lovric and D. Maysinger, J Nanobiotechnology, 5(1), 1, 2007.SJ.

[13] D. Cho, M. Maysinger, B. Jain, B. Roder, S. Hackbarth and F. Winnik, Langmuir, 23(4), 1974-1980, 2007.

[14] G. Oberdorster, Z. Sharp, A. Elder, R. Gelein, W. Kreyling and C. Cox, Inhal Toxicol, 16, 437-445, 2004.

[15] P. Jendelova, V. Herynek, L. Urdzikova, K. Glogarova, J. Kroupova, and B. Andersson, J Neurosci Res, 76, 232-243,2004.

[16] T. Xia, M. Kovochich, J. Brant, M. Hotze, J. Sempf, T. Oberley, C. Sioutas, J. Yeh, M. Wiesner and A. Nel, Nano Lett, 6(8), 1794-807, 2006.

[17] E. Koike and T. Kobayashi, Chemosphere, 65(6), 946-51, 2006.

[18] N. Kedar, J Postgrad Med, 49, 236-245, 2003.

[19] X. Huang, et al., Ann. N. Y. Acad. Sci. 1012, 153-163, 2004.

[20] R. Yokel, J Alzheimers Dis, 10(2-3):223-53, 2006.

[21] P. Adlard and A. Bush, J Alzheimers Dis, 10(2-3):145-63, 2006.

[22] L. Rossi, M. Arciello, C. Capo and G. Rotilio, 55(3-4), 212-21, 2006.